Bergische Universität Wuppertal

Fachbereich Mathematik und Naturwissenschaften

Lehrstuhl für Angewandte Mathematik
und Numerische Mathematik

Preprint BUW-AMNA 08/02

Roland Pulch

Polynomial chaos for multirate partial differential algebraic equations with random parameters

July 2008

http://www-num.math.uni-wuppertal.de

Polynomial Chaos for Multirate Partial Differential Algebraic Equations with Random Parameters

Roland Pulch

Bergische Universität Wuppertal, Fachbereich Mathematik und Naturwissenschaften, Lehrstuhl für Angewandte Mathematik und Numerische Mathematik, Gaußstr. 20, D-42119 Wuppertal, Germany.
Email: pulch@math.uni-wuppertal.de

Abstract

In radio frequency applications, a multivariate model yields an efficient representation of signals with amplitude modulation and/or frequency modulation. Periodic boundary value problems of multirate partial differential algebraic equations (MPDAEs) have to be solved to reproduce the quasiperiodic signals. Typically, technical parameters appear in the system, which may exhibit some uncertainty. Substitution by random variables results in a corresponding stochastic model. We apply the technique of the generalised polynomial chaos to obtain according solutions. A Galerkin approach yields larger coupled systems of MPDAEs. We analyse the properties of the coupled systems with respect to the original formulations. Thereby, we focus on the case of frequency modulation, since the case of amplitude modulation alone is straightforward.

Keywords: differential algebraic equations; multirate partial differential algebraic equations; polynomial chaos; random parameters; uncertainty quantification; Galerkin method; finite difference method.

MSC2000 Subject Classification: 35R60; 35L50; 65N06; 65L80.

1 Introduction

The mathematical modelling of electric circuits is based on network techniques, see [5, 6]. The resulting systems of differential algebraic equations (DAEs) describe the transient behaviour of node voltages and branch currents or possibly additional quantities. In radio frequency applications, the systems exhibit quasiperiodic solutions, where a transient analysis demands a huge computational effort due to the presence of widely separated time scales. A multivariate signal model decouples the time scales and thus enables an efficient representation. Brachtendorf et al. [2] introduced corresponding multirate partial differential algebraic equations (MPDAEs) in case of amplitude modulated signals. Narayan and Roychowdhury [8] formulated warped MPDAEs for frequency modulated signals. In the latter case, the analysis as well as the numerical simulation becomes more complicated, since an appropriate local frequency function is required.

Moreover, the underlying system of DAEs features technical parameters. Some parameters can include uncertainties. In chip design, for example, miniaturisation may cause undesired discrepancies between circuits, which are intended to behave identical. The reason is that capacitive, inductive or resistive components cannot be produced with high precision any more due to the downscaling. Hence it has to be investigated if the circuits still exhibit an acceptable behaviour.

We replace the critical parameters of a given DAE model by random variables to obtain an uncertainty quantification. Thus the corresponding solution of the DAEs becomes a random process. The stochastic model can be resolved by the strategy of the generalised polynomial chaos (gPC) according to [1, 4]. This approach is also suitable for large stochastic perturbations, i.e., we achieve a global sensitivity analysis. On the one hand, the included coefficient functions can be computed approximatively by stochastic collocation, see [15, 16]. On the other hand, a Galerkin approach yields a larger coupled system of DAEs, where the solution represents an approximation of the coefficient functions, see [7].

Considering quasiperiodic signals, the MPDAE formulation includes the same parameters as the underlying system of DAEs. In this article, we apply the approach of the gPC to the MPDAEs, where the Galerkin technique results in larger coupled systems of MPDAEs. It follows that all derived systems inherit a hyperbolic structure from the original MPDAE formulation. In case of pure amplitude modulation, the modelling is straightforward, i.e., the resulting coupled system exhibits the usual form of a system of MPDAEs. However, warped MPDAEs lead to a more sophisticated coupled system in case of frequency modulation, which is not equivalent to a standard system of warped MPDAEs. Thus we focus on the analysis of the latter situation. In particular, we investigate the structure of characteristic curves in the coupled system following [9, 10].

The article is organised as follows. A brief outline of the modelling via MPDAEs is given in Sect. 2. We introduce the technique of the gPC in Sect. 3, where the Galerkin method generates larger coupled systems of MPDAEs. In Sect. 4, we analyse the coupled systems according to warped MPDAEs in detail. Finally, a numerical simulation of a test example based on warped MPDAEs is presented.

2 Multirate Systems

In this section, we summarise the concept of multirate partial differential algebraic equations. For a more detailed description, we refer to [12, 14]. In the following, the required dependence on parameters is already considered in the systems.

2.1 Case of constant time rates

Mathematical modelling of electric circuits yields systems of differential algebraic equations (DAEs), see [5, 6]. We consider DAEs of the form

$$A\frac{\mathrm{d}\mathbf{x}}{\mathrm{d}t} = \mathbf{f}(\mathbf{b}(t), \mathbf{x}(t)), \tag{1}$$

where the time-dependent solution $\mathbf{x} : [t_0, t_1] \to \mathbb{R}^k$ consists of unknown node voltages and branch currents. The right-hand side $\mathbf{f} : \mathbb{R}^l \times \mathbb{R}^k \to \mathbb{R}^k$ includes predetermined input signals $\mathbf{b} : [t_0, t_1] \to \mathbb{R}^l$. If the constant matrix $A \in \mathbb{R}^{k\times k}$ is regular, then the system (1) represents implicit ordinary differential equations (ODEs). In contrast, a singular matrix A implies DAEs.

Technical parameters (capacitances, inductances, resistances, etc.) are included in the system (1). Assuming a tuple of parameters $\mathbf{p} = (p_1, \ldots, p_q) \in \mathbb{R}^q$, the dependence reads

$$A(\mathbf{p})\frac{\mathrm{d}\mathbf{x}}{\mathrm{d}t} = \mathbf{f}(\mathbf{b}(t), \mathbf{x}(t, \mathbf{p}), \mathbf{p}). \tag{2}$$

We consider parameters $\mathbf{p} \in \mathcal{Q}$ belonging to some relevant set $\mathcal{Q} \subseteq \mathbb{R}^q$. Typically, a parameter p_l is present in either the matrix A or the right-hand side $\mathbf{f}$. The input signals $\mathbf{b}$ may also involve parameters. However, the resulting structure agrees to the form (2). We consider quasiperiodic solutions of the system (2).

Definition 1 *A function $x : \mathbb{R} \to \mathbb{C}$ is called m-tone quasiperiodic, if an expansion of the form*

$$x(t) = \sum_{j_1,\ldots,j_m=-\infty}^{+\infty} X_{j_1,\ldots,j_m} \exp\left(\mathrm{i}2\pi\left(\frac{j_1}{T_1} + \cdots + \frac{j_m}{T_m}\right)t\right) \tag{3}$$

exists, where $X_{j_1,\ldots,j_m} \in \mathbb{C}$ *are constant coefficients. In this representation,* m *time rates* $T_1, \ldots, T_m > 0$ *are given, which are not necessarily incommensurable.*

We assume an absolute convergence of the series (3). Furthermore, we restrict to the most frequent case of two-tone quasiperiodic functions. Let the input signals $\mathbf{b}$ be two-tone quasiperiodic. Often the solution of (2) inherits the transient behaviour of the input signals. Thus we assume the representation

$$\mathbf{x}(t, \mathbf{p}) = \sum_{j_1, j_2 = -\infty}^{+\infty} \mathbf{X}_{j_1, j_2}(\mathbf{p}) \exp\left(\mathrm{i}2\pi \left(\frac{j_1}{T_1} + \frac{j_2}{T_2}\right) t\right) \tag{4}$$

with coefficients $\mathbf{X}_{j_1,j_2}(\mathbf{p}) \in \mathbb{C}^k$ for each parameter $\mathbf{p} \in \mathcal{Q}$.

Typically, quasiperiodic signals represent oscillations. Let (w.l.o.g.) $T_1 \geq T_2$. In radio frequency applications, the time rates T_1, T_2 are widely separated, i.e., it holds $T_1 \gg T_2$. A numerical integration of the system (2) for a fixed tuple of parameters becomes inefficient, since the fast rate T_2 restricts the step size in time, whereas the slow rate T_1 determines the total time interval of the simulation.

Alternatively, the structure of quasiperiodic signals (3) implies a natural representation by assigning an own variable for each separate time scale. The corresponding multivariate function (MVF) reads

$$\hat{x}(t_1, \ldots, t_m) = \sum_{j_1, \ldots, j_m = -\infty}^{+\infty} X_{j_1,\ldots,j_m} \exp\left(\mathrm{i}2\pi \left(\frac{j_1 t_1}{T_1} + \cdots + \frac{j_m t_m}{T_m}\right)\right), \tag{5}$$

which is periodic in each independent variable with the periods $T_1, \ldots, T_m$. The original signal (3) can be reconstructed completely from its MVF (5) via

$$x(t) = \hat{x}(t, \ldots, t). \tag{6}$$

Accordingly, the solution (4) exhibits the biperiodic representation

$$\hat{\mathbf{x}}(t_1, t_2, \mathbf{p}) = \sum_{j_1, j_2 = -\infty}^{+\infty} \mathbf{X}_{j_1, j_2}(\mathbf{p}) \exp\left(\mathrm{i}2\pi \left(\frac{j_1 t_1}{T_1} + \frac{j_2 t_2}{T_2}\right)\right) \tag{7}$$

for each tuple $\mathbf{p} \in \mathcal{Q}$. The periodicities allow for sampling the MVFs in the rectangular domain $[0, T_1] \times [0, T_2]$. Typically, the MVFs feature a simple structure in this rectangle. Hence the MVFs can be resolved on a relatively coarse grid in time domain.

Now the idea is to compute the MVFs (7) instead of the original signals (4), since the reconstruction (6) yields the desired information. Replacing the input signals as well as the solution of (2) by MVFs changes the DAE model into multirate partial differential algebraic equations introduced by Brachtendorf et al. [2].

Definition 2 *The multirate partial differential algebraic equations (MPDAEs) corresponding to the system of DAEs (2) read*

$$A(\mathbf{p})\left(\frac{\partial \hat{\mathbf{x}}}{\partial t_1}+\frac{\partial \hat{\mathbf{x}}}{\partial t_2}\right)=\mathbf{f}(\hat{\mathbf{b}}(t_1,t_2),\hat{\mathbf{x}}(t_1,t_2,\mathbf{p}),\mathbf{p}), \tag{8}$$

where $\hat{\mathbf{b}}:\mathbb{R}^2\to\mathbb{R}^k$ *and* $\hat{\mathbf{x}}:\mathbb{R}^2\times\mathcal{Q}\to\mathbb{R}^k$ *are MVFs.*

It is straightforward to verify that a biperiodic solution of the MPDAEs (8) yields a two-tone quasiperiodic solution of the DAEs (2) in the reconstruction (6).

2.2 Case of frequency modulation

We assume the presence of two separated time scales in the system of DAEs (2) again. However, the input signals $\mathbf{b}$ are just periodic with slow time rate T_1 now. The solution $\mathbf{x}$ inherits this forced oscillation. In addition, let the solution exhibit a fast autonomous oscillation. The frequency of the fast oscillation is modulated slowly in time by the input signals. The resulting signals are quasiperiodic and show a representation

$$\mathbf{x}(t,\mathbf{p})=\sum_{j_1,j_2=-\infty}^{+\infty}\mathbf{X}_{j_1,j_2}(\mathbf{p})\exp\left(\mathrm{i}2\pi\left(\frac{j_1}{T_1}+\frac{j_2}{T_2(\mathbf{p})}\right)t\right). \tag{9}$$

Remark that the fast rate T_2 depends on the parameters in (2) now. A biperiodic MVF (7) of the signal (9) exists again. However, this representation is inefficient in general, since many oscillations occur in the domain $[0,T_1]\times[0,T_2]$. Narayan and Roychowdhury [8] introduced an alternative modelling via a $(T_1,1)$-periodic MVF $\hat{\mathbf{x}}:\mathbb{R}^2\to\mathbb{R}^k$ and a local frequency function $\nu:\mathbb{R}\to\mathbb{R}$. The corresponding reconstruction of the signal reads

$$\mathbf{x}(t,\mathbf{p})=\hat{\mathbf{x}}(t,\Psi(t,\mathbf{p}),\mathbf{p})\qquad\text{with}\qquad\Psi(t,\mathbf{p})=\int_0^t\nu(s,\mathbf{p})\,\mathrm{d}s, \tag{10}$$

where ν represents a local frequency. The function ν includes the magnitude of the fast time scale and thus depends on the parameters. The warping function Ψ stretches the second time scale in the MVF. An appropriate local frequency function is unknown a priori. Again the introduction of MVFs yields a corresponding MPDAE model, see [8].

Definition 3 *The system of warped multirate partial differential algebraic equations (wMPDAEs) corresponding to the system of DAEs (2) is given by*

$$A(\mathbf{p})\left(\frac{\partial \hat{\mathbf{x}}}{\partial t_1}+\nu(t_1,\mathbf{p})\frac{\partial \hat{\mathbf{x}}}{\partial t_2}\right)=\mathbf{f}(\mathbf{b}(t_1),\hat{\mathbf{x}}(t_1,t_2,\mathbf{p}),\mathbf{p}) \tag{11}$$

with MVF $\hat{\mathbf{x}}:\mathbb{R}^2\times\mathcal{Q}\to\mathbb{R}^k$ *and local frequency function* $\nu:\mathbb{R}\times\mathcal{Q}\to\mathbb{R}$.

We do not need a MVF for the input signals $\mathbf{b}$ due to the presence of the slow time scale only. The local frequency function depends on the variable t_1, since the frequency modulation is caused by the input signals. It can be shown that a pair $\hat{\mathbf{x}}, \nu$ satisfying the wMPDAE (11) yields a quasiperiodic solution of the DAEs (2) via the reconstruction (10).

An appropriate local frequency function is unknown a priori, i.e., the system (11) is underdetermined. According to [13], the existence of a representation (9) implies that each continuous T_1-periodic function ν is feasible, which satisfies

$$\frac{1}{T_1} \int_0^{T_1} \nu(s, \mathbf{p}) \, \mathrm{d}s = \frac{1}{T_2(\mathbf{p})}. \tag{12}$$

Nevertheless, the corresponding pairs $\hat{\mathbf{x}}, \nu$ reproduce the same solution of the DAEs (2) in the reconstruction (10).

We require an additional condition to determine an appropriate local frequency function. Continuous phase conditions are able to identify efficient representations in general, see [8, 11]. For example, the property

$$\hat{x}_1(t_1, 0) = \eta(t_1) \qquad \text{for all } \; t_1 \in \mathbb{R} \tag{13}$$

is imposed on the (w.l.o.g.) first component of the MVF $\hat{\mathbf{x}} = (\hat{x}_1, \ldots, \hat{x}_k)^\top$, where a predetermined slowly varying function $\eta : \mathbb{R} \to \mathbb{R}$ is used. Often a constant choice $\eta(t_1) \equiv \eta_0$ is adequate. Likewise, the condition

$$\frac{\partial \hat{x}_1}{\partial t_2}(t_1, 0) = 0 \qquad \text{for all } \; t_1 \in \mathbb{R} \tag{14}$$

can be applied. These continuous phase conditions represent additional boundary conditions in time domain. The system (11) is autonomous in the variable t_2. Thus a family of translated solutions exists for each local frequency function. Phase conditions like (13) or (14) are able to isolate a particular solution.

3 Application of Polynomial Chaos

In the system (2), we assume that the selected parameters exhibit some uncertainty. We replace the parameters by random variables. The resulting multirate systems with stochastic parameters can be resolved by quasi Monte-Carlo methods, for example. Alternatively, we apply the approach of the generalised polynomial chaos (gPC), which represents a spectral method, see [4], and thus utilises more structure of the random solution. The gPC approach also yields a possibility to verify results obtained by standard techniques like quasi Monte-Carlo methods, multidimensional quadrature or others.

3.1 Preliminaries

We assume (w.l.o.g.) that the tuples $\mathbf{p} \in \mathcal{Q} \subseteq \mathbb{R}^q$ include just the parameters to be analysed with respect to uncertainties. We substitute the parameters by random variables

$$\boldsymbol{\xi} : \Omega \to \mathcal{Q}, \quad \boldsymbol{\xi} = (\xi_1, \ldots, \xi_q)^\top$$

corresponding to some probability space $(\Omega, \mathcal{A}, P)$. Let each random variable ξ_i exhibit a classical distribution (uniform, beta, Gaussian, etc.). Given a measurable function $f : \mathbb{R}^q \to \mathbb{R}$ depending on the random variables, the expected value reads (if exists)

$$\langle f \rangle := \int_\Omega f(\boldsymbol{\xi}(\omega)) \, \mathrm{d}P(\omega) = \int_{\mathbb{R}^q} f(\boldsymbol{\xi}) \rho(\boldsymbol{\xi}) \, \mathrm{d}\boldsymbol{\xi}, \tag{15}$$

where $\rho : \mathbb{R}^q \to \mathbb{R}$ represents the density function of the random parameters. We assume that the expected value exists for all polynomials. Accordingly, the inner product of two functions $f, g : \mathbb{R}^q \to \mathbb{R}$ implies the formula (if exists)

$$\langle fg \rangle := \int_\Omega f(\boldsymbol{\xi}(\omega)) g(\boldsymbol{\xi}(\omega)) \, \mathrm{d}P(\omega) = \int_{\mathbb{R}^q} f(\boldsymbol{\xi}) g(\boldsymbol{\xi}) \rho(\boldsymbol{\xi}) \, \mathrm{d}\boldsymbol{\xi}. \tag{16}$$

We apply the expected value also to vector-valued as well as matrix-valued functions by components.

Substitution of the parameters by random variables changes the deterministic solution of the DAEs (2) into a random process

$$\mathbf{y} : [t_0, t_1] \times \Omega \to \mathbb{R}^k, \qquad \mathbf{y}(t, \omega) = \mathbf{x}(t, \boldsymbol{\xi}(\omega)).$$

We are interested in key data of the process like the expected value and the variance, for example. Nevertheless, more complicated information can be considered.

Observing a solution of the DAEs (2), differential components have to be smooth in time, whereas algebraic components are just required to be continuous. For simplicity, we assume that all components are smooth with respect to time, i.e.,

$$\mathbf{x}(\cdot, \boldsymbol{\xi}(\omega)) \in C^1([t_0, t_1]) \qquad \text{for almost all } \omega \in \Omega.$$

Furthermore, we demand finite second moments of the stochastic process

$$\langle x_j(t, \boldsymbol{\xi})^2 \rangle < \infty \qquad \text{for each } t \in [t_0, t_1] \tag{17}$$

and all $j = 1, \ldots, k$ with $\mathbf{x} = (x_1, \ldots, x_k)^\top$. It follows that the stochastic process exhibits the expansion

$$\mathbf{x}(t, \boldsymbol{\xi}(\omega)) = \sum_{i=0}^{\infty} \mathbf{v}_i(t) \Phi_i(\xi_1(\omega), \ldots, \xi_q(\omega)), \tag{18}$$

where the functions $(\Phi_i)_{i\in\mathbb{N}}$, $\Phi_i : \mathbb{R}^q \to \mathbb{R}$ represent a complete basis of polynomials. We apply an orthonormal system in the following, i.e., $\langle \Phi_i \Phi_j \rangle = \delta_{ij}$ holds with the Kronecker-delta. The coefficient functions $\mathbf{v}_i : [t_0, t_1] \to \mathbb{R}^k$ satisfy the relation

$$\mathbf{v}_i(t) = \langle \Phi_i(\boldsymbol{\xi}) \mathbf{x}(t, \boldsymbol{\xi}) \rangle. \tag{19}$$

The convergence of the series (18) proceeds in $L^2(\Omega)$, i.e.,

$$\lim_{n\to\infty} \left\langle \left(x_j(t, \boldsymbol{\xi}) - \sum_{i=0}^{n} v_{i,j}(t) \Phi_i(\boldsymbol{\xi}) \right)^2 \right\rangle = 0 \qquad \text{for each } \ t \tag{20}$$

and all components $j = 1, \ldots, k$, where $\mathbf{v}_i = (v_{i,1}, \ldots, v_{i,k})^\top$.

If the random variables $\boldsymbol{\xi}$ are Gaussian, then the orthonormal basis consists of the Hermite polynomials. The corresponding approach is called the (homogeneous) polynomial chaos. If some random variable is non-Gaussian, then we obtain the technique of the generalised polynomial chaos (gPC). For more details on the approach of gPC, we refer to [1, 4, 7].

Due to the definition of the inner product (16), the coefficient functions are specified by parameter-dependent integrals (19), where the time represents the parameter. Given a density function ρ with compact support, it follows directly that the functions $\mathbf{v}_i$ are smooth provided that $\mathbf{x}$ is smooth in time and all involved functions are piecewise continuous with respect to the parameters $\mathbf{p}$. If the support of the density function is not bounded or if significant discontinuities are present, then an integrable function dominating the derivatives of $\mathbf{x}$ is required to ensure the smoothness of the coefficient functions. The latter case appears for random variables $\boldsymbol{\xi}$ with Gaussian distributions, for example.

Considering the DAEs (2) with stochastic parameters, the coefficient functions $\mathbf{v}_i$ of the stochastic process (18) are unknown a priori. The integrals (19) can be evaluated approximately via stochastic collocation, see [15, 16]. Thereby, multidimensional Gaussian quadrature can be used based on the tensor product of the one-dimensional formula. In higher dimensions, Monte-Carlo methods, quasi-Monte-Carlo methods or sparse grids are more adequate. Each evaluation of the integrand in (19) for a particular value $\boldsymbol{\xi}$ demands a numerical simulation of the system of DAEs (2).

Alternatively, we construct a numerical method based on a Galerkin approach following [7]. We truncate the expansion (18) at the mth term

$$\mathbf{x}^{(m)}(t, \boldsymbol{\xi}(\omega)) = \sum_{i=0}^{m} \mathbf{v}_i(t) \Phi_i(\xi_1(\omega), \ldots, \xi_q(\omega)). \tag{21}$$

Corresponding approximations of the expected value and the variance are determined via

$$\begin{aligned} \langle \mathbf{x}(t,\boldsymbol{\xi})\rangle &\doteq \langle \mathbf{x}^{(m)}(t,\boldsymbol{\xi})\rangle = \mathbf{v}_0(t), \\ \mathrm{Var}(x_j(t,\boldsymbol{\xi})) &\doteq \mathrm{Var}(x_j^{(m)}(t,\boldsymbol{\xi})) = \sum_{i=1}^{m} v_{i,j}(t)^2 \end{aligned} \tag{22}$$

in each time point $t \in [t_0, t_1]$. Nevertheless, other quantities may be required, which can often be reconstructed from the coefficient functions.

Inserting the approximation (21) into the system (2) yields the residual

$$\mathbf{r}(t,\boldsymbol{\xi}) = A(\boldsymbol{\xi}) \left(\frac{\mathrm{d}}{\mathrm{d}t} \sum_{i=0}^{m} \mathbf{v}_i(t)\Phi_i(\boldsymbol{\xi}) \right) - \mathbf{f}\left(\mathbf{b}(t), \sum_{i=0}^{m} \mathbf{v}_i(t)\Phi_i(\boldsymbol{\xi}), \boldsymbol{\xi} \right).$$

To determine the unknown coefficient functions, we apply the Galerkin method, i.e., we demand

$$\langle \Phi_l(\boldsymbol{\xi})\mathbf{r}(t,\boldsymbol{\xi})\rangle = \mathbf{0} \qquad \text{for each } \ t \in [t_0,t_1] \ \text{ and } \ l = 0,1,\ldots,m.$$

Accordingly, we achieve a larger coupled system of DAEs.

Definition 4 *The gPC system of DAEs corresponding to (2) obtained by a Galerkin approach reads*

$$\sum_{i=0}^{m} \langle \Phi_l(\boldsymbol{\xi})\Phi_i(\boldsymbol{\xi})A(\boldsymbol{\xi})\rangle \frac{\mathrm{d}\mathbf{v}_i}{\mathrm{d}t} = \left\langle \Phi_l(\boldsymbol{\xi})\mathbf{f}\left(\mathbf{b}(t), \sum_{i=0}^{m} \mathbf{v}_i(t)\Phi_i(\boldsymbol{\xi}), \boldsymbol{\xi} \right) \right\rangle \tag{23}$$

for $l = 0,1,\ldots,m$.

Although the coefficients satisfying the system (23) are not identical to the functions in (18), we employ the same symbol for convenience. If the matrix A does not depend on the parameters, then the system (23) simplifies to

$$A\frac{\mathrm{d}\mathbf{v}_l}{\mathrm{d}t} = \left\langle \Phi_l(\boldsymbol{\xi})\mathbf{f}\left(\mathbf{b}(t), \sum_{i=0}^{m} \mathbf{v}_i(t)\Phi_i(\boldsymbol{\xi}), \boldsymbol{\xi} \right) \right\rangle$$

for $l = 0,1,\ldots,m$ in view of the orthonormal basis polynomials.

We comment shortly on the case of large numbers q of random parameters. The basis polynomials depend on q independent variables. Thus the number of polynomials up to a certain degree d increases rapidly due to $m+1 = (q+d)!/(q!d!)$. Further techniques have to be applied for reducing the problem size of the large coupled systems in case of many parameters, which corresponds to a model order

reduction. Methods based on ANOVA (analysis of variance) expansions enable a promising strategy, see for example [3]. If the input for the DAEs (1) is a time-dependent random process, then it can be represented by a Karhunen-Loève expansion, see [4]. Truncating this expansion yields a finite set of random variables and the above approach becomes feasible, cf. [7]. The number of required variables for a sufficiently accurate approximation depends on the correlation length of the random process.

3.2 Case of constant time rates

Now we assume that a two-tone quasiperiodic solution of the DAE system (2) exists for each tuple of parameters, where the widely separated time rates T_1, T_2 are forced by the input signals. Thus we consider the MPDAE (8) with stochastic parameters. The according biperiodic solution becomes a random field

$$\hat{\mathbf{y}} : [0, T_1] \times [0, T_2] \times \Omega \to \mathbb{R}^k, \qquad \hat{\mathbf{y}}(t_1, t_2, \omega) = \hat{\mathbf{x}}(t_1, t_2, \boldsymbol{\xi}(\omega)).$$

We assume finite second moments

$$\langle \hat{x}_j(t_1, t_2, \boldsymbol{\xi})^2 \rangle < \infty \qquad \text{for each } \ t_1, t_2 \tag{24}$$

and all $j = 1, \ldots, k$ with $\hat{\mathbf{x}} = (\hat{x}_1, \ldots, \hat{x}_k)^\top$. The condition (24) of the MPDAE solution implies finite second moments (17) of the reconstructed DAE solution.

Consequently, the MVF seen as a random field owns the representation

$$\hat{\mathbf{x}}(t_1, t_2, \boldsymbol{\xi}(\omega)) = \sum_{i=0}^{\infty} \hat{\mathbf{v}}_i(t_1, t_2) \Phi_i(\xi_1(\omega), \ldots, \xi_q(\omega)) \tag{25}$$

with convergence in $L^2(\Omega)$ for each t_1, t_2 analogue to (20). The basis polynomials $(\Phi_i)_{i \in \mathbb{N}}$ are identical to the functions in (18). The coefficient functions $\hat{\mathbf{v}}_i : [0, T_1] \times [0, T_2] \to \mathbb{R}^k$ are specified by the relation

$$\hat{\mathbf{v}}_i(t_1, t_2) = \langle \Phi_i(\boldsymbol{\xi}) \hat{\mathbf{x}}(t_1, t_2, \boldsymbol{\xi}) \rangle. \tag{26}$$

Accordingly, smoothness of the coefficient functions follows from the properties of the involved functions, cf. (19).

We apply a finite number of terms in (25) again, which results in the residual corresponding to (8)

$$\begin{aligned} \mathbf{r}(t_1, t_2, \boldsymbol{\xi}) \ &= \ A(\boldsymbol{\xi}) \left(\frac{\partial}{\partial t_1} + \frac{\partial}{\partial t_2} \right) \sum_{i=0}^{m} \hat{\mathbf{v}}_i(t_1, t_2) \Phi_i(\boldsymbol{\xi}) \\ &\quad - \mathbf{f} \left(\hat{\mathbf{b}}(t_1, t_2), \sum_{i=0}^{m} \hat{\mathbf{v}}_i(t_1, t_2) \Phi_i(\boldsymbol{\xi}), \boldsymbol{\xi} \right). \end{aligned}$$

Now the Galerkin method yields a larger coupled system of MPDAEs.

Definition 5 *The gPC system of MPDAEs corresponding to (8), which is constructed by a Galerkin method, is given by*

$$\begin{aligned} &\sum_{i=0}^{m} \langle \Phi_l(\boldsymbol{\xi}) \Phi_i(\boldsymbol{\xi}) A(\boldsymbol{\xi}) \rangle \left(\frac{\partial \hat{\mathbf{v}}_i}{\partial t_1} + \frac{\partial \hat{\mathbf{v}}_i}{\partial t_2} \right) \\ = \; &\left\langle \Phi_l(\boldsymbol{\xi}) \mathbf{f} \left(\hat{\mathbf{b}}(t_1, t_2), \sum_{i=0}^{m} \hat{\mathbf{v}}_i(t_1, t_2) \Phi_i(\boldsymbol{\xi}), \boldsymbol{\xi} \right) \right\rangle \end{aligned} \tag{27}$$

for $l = 0, 1, \ldots, m$.

The dimension of the system (27) is $k(m+1)$. The system has the form of a larger MPDAE (8) with particular matrix and right-hand side. The coefficient functions $\hat{\mathbf{v}}_i$ inherit the periodicities of the random field $\hat{\mathbf{x}}$ due to (26). Thus a method of characteristics solves the biperiodic boundary value problem efficiently, see [9].

Alternatively, we consider the gPC system of DAEs (23). The involved coefficients inherit the time behaviour of the solutions of the original system (2) in view of (19). Hence the coefficient functions $\mathbf{v}_i$ are two-tone quasiperiodic with rates T_1, T_2 forced by the input signals. We apply the concept of MVFs and derive the system of MPDAEs corresponding to the DAEs (23). Thereby, we obtain exactly the system (27).

The mathematical modelling is illustrated in Fig. 1. Two options yield the same system of coupled MPDAEs (27), namely by performing the steps (a),(b) or the steps (c),(d). We recognise that the steps (b) and (c) correspond to an approximation in the stochastic model, where the random parameters are eliminated by integration.

Furthermore, we remark one particular advantage in solving biperiodic problems of the larger systems (27) in comparison to computing the coefficients (26) by stochastic collocation. On the one hand, each evaluation of the integrand in (26) demands the solution of a biperiodic problem of the MPDAE system (8). Newton iterations yield numerical solutions for these boundary value problems. To be efficient, previously computed solutions have to be used as starting values for neighbouring problems. Thus we require a sophisticated ordering of the involved parameter values. Furthermore, a failure of convergence is possible due to insufficient starting values. We have to apply continuation methods with respect to the parameters in case of failure. The implementation of corresponding algorithms becomes extensive for two or more random parameters. On the other hand, the biperiodic problem of the coupled MPDAEs (27) implies just one large nonlinear system in a numerical method. Hence we have to control the convergence of just a single Newton iteration. Note that the approach via stochastic collocation can still be efficient provided that sophisticated algorithms are implemented.

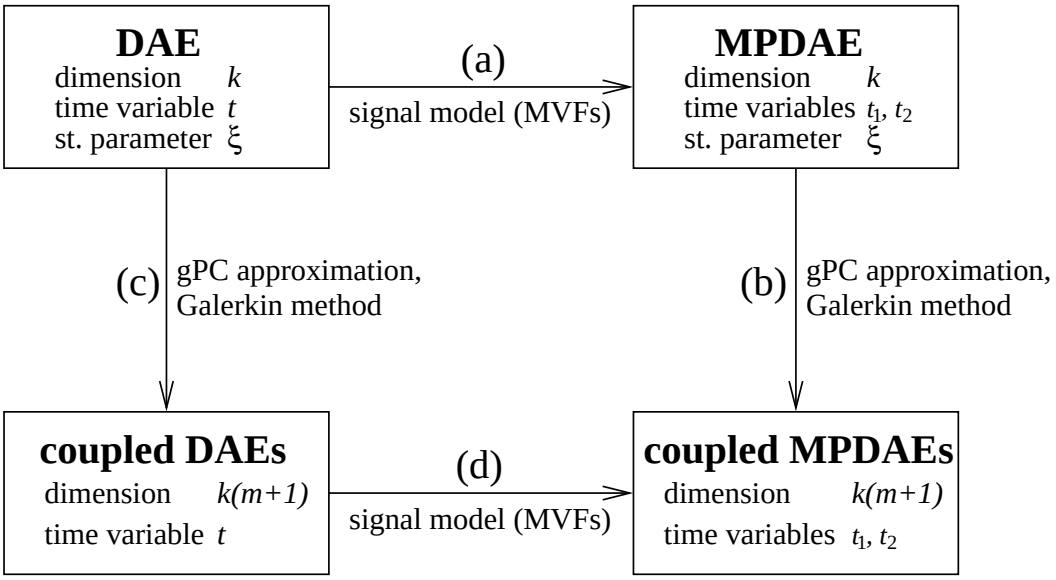

Figure 1: Interaction between MPDAE approach and Polynomial Chaos.

3.3 Case of frequency modulation

The modelling becomes more complex for frequency modulated signals. In the previous case, the input signals force the time rates T_1, T_2. Hence all two-tone quasiperiodic solutions exhibit identical time rates. In contrast, the input signals imply just the slow rate T_1 now. The solutions of (2) are quasiperiodic functions (9), where the time rate T_2 depends on the stochastic parameters. It follows that the option (d) in Fig. 1 is not feasible, since the signal model applies a particular local frequency function for all components of the solution. However, the relation (12) shows that each local frequency function is associated with a fast time rate T_2. A single local frequency is feasible if the fast rates are identical for all parameters, which is not given in general. Numerical simulations confirm this fact, since corresponding Newton iterations do not converge in finite difference methods used successfully in [13].

Consequently, we apply the system of wMPDAEs (11), which is achieved by step (a) in Fig. 1. We assume that the solutions exhibit the expansion (25) guaranteed by finite second moments (24). The time domain is standardised to $[0, T_1] \times [0, 1]$. Since the local frequency function depends on the stochastic parameters, we consider pointwise finite second moments and apply

$$\nu(t_1, \boldsymbol{\xi}(\omega)) = \sum_{i=0}^{\infty} w_i(t_1) \Phi_i(\xi_1(\omega), \ldots, \xi_q(\omega)) \tag{28}$$

with T_1-periodic coefficients $w_i : \mathbb{R} \to \mathbb{R}$ and the same basis polynomials as

in (25). Inserting the finite approximations of (25) as well as (28) in the system of wMPDAEs (11), we obtain the residual

$$\begin{aligned}\mathbf{r}(t_1,t_2,\boldsymbol{\xi}) &= A(\boldsymbol{\xi})\left(\frac{\partial}{\partial t_1}+\left(\sum_{j=0}^{m'} w_j(t_1)\Phi_j(\boldsymbol{\xi})\right)\frac{\partial}{\partial t_2}\right)\sum_{i=0}^{m}\hat{\mathbf{v}}_i(t_1,t_2)\Phi_i(\boldsymbol{\xi}) \\ &\quad -\mathbf{f}\left(\mathbf{b}(t_1),\sum_{i=0}^{m}\hat{\mathbf{v}}_i(t_1,t_2)\Phi_i(\boldsymbol{\xi}),\boldsymbol{\xi}\right).\end{aligned}$$

Again the Galerkin technique provides us a coupled system of MPDAEs subject to the condition $m = m'$.

Definition 6 *The gPC system of wMPDAEs corresponding to (11) achieved by a Galerkin approach reads*

$$\begin{aligned}&\sum_{i=0}^{m}\left[\langle\Phi_l(\boldsymbol{\xi})\Phi_i(\boldsymbol{\xi})A(\boldsymbol{\xi})\rangle\frac{\partial\hat{\mathbf{v}}_i}{\partial t_1}+\sum_{j=0}^{m}\langle\Phi_l(\boldsymbol{\xi})\Phi_i(\boldsymbol{\xi})\Phi_j(\boldsymbol{\xi})A(\boldsymbol{\xi})\rangle w_j(t_1)\frac{\partial\hat{\mathbf{v}}_i}{\partial t_2}\right] \\ =\ &\left\langle\Phi_l(\boldsymbol{\xi})\mathbf{f}\left(\mathbf{b}(t_1),\sum_{i=0}^{m}\hat{\mathbf{v}}_i(t_1,t_2)\Phi_i(\boldsymbol{\xi}),\boldsymbol{\xi}\right)\right\rangle\end{aligned} \tag{29}$$

for $l = 0, 1, \ldots, m$.

We recognise that the left-hand side of (29) becomes more complicated in comparison to (11) or (27). Moreover, we encounter $m+1$ unknown coefficient functions w_j in the system (29). Again the phase conditions provide us additional information to solve the complete system. According to (13), we demand

$$\hat{x}_1(t_1,0,\boldsymbol{\xi}) = \eta(t_1,\boldsymbol{\xi}) \quad \text{for all } t_1 \text{ and each } \boldsymbol{\xi}$$

using a predetermined function η. A corresponding Galerkin projection yields the conditions

$$\hat{v}_{i,1}(t_1,0) = \langle\eta(t_1,\boldsymbol{\xi})\Phi_i(\boldsymbol{\xi})\rangle \quad \text{for all } t_1 \text{ and } i = 0,1,\ldots,m.$$

A constant choice $\eta(t_1,\boldsymbol{\xi}) \equiv \eta_0$ is often feasible, where the requirements simplify to

$$\hat{v}_{0,1}(t_1,0) = \eta_0 \qquad \text{and} \qquad \hat{v}_{i,1}(t_1,0) = 0 \quad \text{for } i = 1,\ldots,m \tag{30}$$

including all t_1. Likewise, the condition (14) implies

$$\frac{\partial\hat{v}_{i,1}}{\partial t_2}(t_1,0) = 0 \quad \text{for all } t_1 \text{ and } i = 0,1,\ldots,m.$$

The additional relations are used to achieve as many equations as unknowns in a suitable numerical method.

We note that the reconstruction of solutions of the DAEs (2) by a solution of the gPC system of wMPDAEs (29) becomes more involved than in the original case. According to (10), the reconstruction reads

$$\mathbf{x}(t,\boldsymbol{\xi}) \doteq \sum_{i=0}^{m} \hat{\mathbf{v}}_i \left(t, \sum_{j=0}^{m} \Phi_j(\boldsymbol{\xi}) \int_0^t w_j(s)\, \mathrm{d}s \right) \Phi_i(\boldsymbol{\xi}).$$

Thus the computation of expected value and variance is not straightforward. Nevertheless, a cheap sampling in random space is feasible provided that the coefficient functions have already been calculated. Moreover, properties of the quasiperiodic DAE solutions can often be illustrated by an investigation of the MPDAE solutions alone.

4 Analysis of Warped Systems

In this section, we analyse the system (29) of the gPC for wMPDAEs further. For the sake of shortness, we consider a constant matrix A. The following results are also valid, if the matrix A is block diagonal and all random parameters belong to invertible minors. The system (29) simplifies to

$$A \left[\frac{\partial \hat{\mathbf{v}}_l}{\partial t_1} + \sum_{i,j=0}^{m} \langle \Phi_l(\boldsymbol{\xi}) \Phi_i(\boldsymbol{\xi}) \Phi_j(\boldsymbol{\xi}) \rangle w_j(t_1) \frac{\partial \hat{\mathbf{v}}_i}{\partial t_2} \right] = \mathbf{F}_l(\mathbf{b}(t_1), \hat{\mathbf{v}}(t_1,t_2)) \tag{31}$$

for $l = 0, 1, \ldots, m$, where an abbreviation is used for the right-hand side and $\hat{\mathbf{v}} := (\hat{\mathbf{v}}_0^\top, \ldots, \hat{\mathbf{v}}_m^\top)^\top$. Using Kronecker products, we write the complete system as

$$(I_{m+1} \otimes A) \frac{\partial \hat{\mathbf{v}}}{\partial t_1} + (B(t_1) \otimes A) \frac{\partial \hat{\mathbf{v}}}{\partial t_2} = \mathbf{F}(\mathbf{b}(t_1), \hat{\mathbf{v}}(t_1,t_2)) \tag{32}$$

with the identity matrix $I_{m+1} \in \mathbb{R}^{(m+1)\times(m+1)}$ and the matrix

$$B(t_1) := \sum_{j=0}^{m} w_j(t_1) M_j \in \mathbb{R}^{(m+1)\times(m+1)}, \tag{33}$$

which includes the functions with respect to the local frequencies. The constant matrices

$$M_l := (\mu_{lij}) \in \mathbb{R}^{(m+1)\times(m+1)}, \qquad \mu_{lij} := \langle \Phi_l \Phi_i \Phi_j \rangle \qquad \text{for } l = 0, 1, \ldots, m$$

consist of expected values. Thereby, the coefficients μ_{lij} are symmetric in all indices. The basis polynomial $\Phi_0 \equiv 1$ causes $M_0 = I_{m+1}$ due to $\langle \Phi_i \Phi_j \rangle = \delta_{ij}$.

The matrices (33) are symmetric for each t_1, since the matrices M_l are symmetric. Thus a transformation to a diagonal matrix

$$B(t_1) = S(t_1)^\top \Lambda(t_1) S(t_1) \tag{34}$$

exists using orthogonal matrices $S(t_1) \in \mathbb{R}^{(m+1)\times(m+1)}$. It is obvious to ask for the definiteness of the matrices (33). In the model (11), negative local frequencies are feasible. However, the presence of widely separated time scales implies a strictly positive local frequency function. Accordingly, characteristic curves of (11) exhibit a certain direction, see [10]. The deterministic case (11) corresponds to the choice $w_j(t_1) \equiv 0$ for $j > 0$, where $B(t_1) \equiv w_0(t_1) I_{m+1}$ holds and thus the matrix is positive definite for $w_0(t_1) > 0$. Assuming small stochastic perturbations, we achieve the following generalisation.

Theorem 1 *Given T_1-periodic functions w_j for $j = 0, 1, \ldots, m$, let $w_0(t_1) > 0$ for all t_1. If*

$$(m+1) \left(\max_{0 \le i \le m} \sqrt{\langle \Phi_i^4 \rangle} \right) \sum_{j=1}^{m} |w_j(t_1)| < w_0(t_1)$$

holds for all t_1, then the symmetric matrices $B(t_1) \in \mathbb{R}^{(m+1)\times(m+1)}$ in (33) are positive definite.

Proof:

Let $\lambda \in \mathbb{R}$ be an arbitrary eigenvalue of the matrix $B(t_1)$. We apply the structure

$$B(t_1) = w_0(t_1) I_{m+1} + \sum_{j=1}^{m} w_j(t_1) M_j,$$

where the latter sum represents a perturbation of the diagonal matrix $w_0 I_{m+1}$. The Bauer-Fike theorem implies

$$\begin{aligned} |\lambda - w_0(t_1)| &\le \left\| \sum_{j=1}^{m} w_j(t_1) M_j \right\|_p \le \sum_{j=1}^{m} |w_j(t_1)| \cdot \|M_j\|_p \\ &\le \left(\max_{1 \le l \le m} \|M_l\|_p \right) \sum_{j=1}^{m} |w_j(t_1)| \end{aligned}$$

in an arbitrary p-norm. The Cauchy-Schwarz inequality for the inner product (16) yields together with $\langle \Phi_l^2 \rangle = 1$

$$\begin{aligned} \|M_l\|_\infty &= \max_{0 \le i \le m} \sum_{j=0}^{m} |\langle \Phi_l \Phi_i \Phi_j \rangle| \le (m+1) \max_{0 \le i,j \le m} |\langle \Phi_l \Phi_i \Phi_j \rangle| \\ &\le (m+1) \max_{0 \le i,j \le m} \sqrt{\langle \Phi_l^2 \rangle \langle \Phi_i^2 \Phi_j^2 \rangle} \le (m+1) \max_{0 \le i,j \le m} \sqrt[4]{\langle \Phi_i^4 \rangle \langle \Phi_j^4 \rangle}, \end{aligned}$$

where the estimate is independent of the number l. The assumed property implies $|\lambda - w_0(t_1)| < w_0(t_1)$ and thus it holds $\lambda > 0$. □

Hence the matrices (33) inherit the positive definiteness of the matrix in the deterministic case provided that the variances are sufficiently small.

Solutions of the wMPDAE system (11) exhibit a degree of freedom by transformations, see [13]. In case of the gPC system (31), the following transformation is feasible.

Theorem 2 *Let $\hat{\mathbf{v}}_0, \ldots, \hat{\mathbf{v}}_m$ be a $(T_1, 1)$-periodic solution of the system (31) including the T_1-periodic functions $w_0, \ldots, w_m$. Applying a T_1-periodic function $\bar{w}_0 : \mathbb{R} \to \mathbb{R}$, we define the MVFs*

$$\bar{\mathbf{v}}_l(t_1, t_2) := \hat{\mathbf{v}}_l \left(t_1, t_2 + \int_0^{t_1} w_0(s) - \bar{w}_0(s) \, \mathrm{d}s \right) \tag{35}$$

for $l = 0, 1, \ldots, m$. It follows that the MVFs $\bar{\mathbf{v}}_0, \ldots, \bar{\mathbf{v}}_m$ solve the system (31) with the functions $\bar{w}_0, w_1, \ldots, w_m$. If the condition

$$\int_0^{T_1} w_0(s) \, \mathrm{d}s = \int_0^{T_1} \bar{w}_0(s) \, \mathrm{d}s \tag{36}$$

holds for the average, then the MVFs $\bar{\mathbf{v}}_0, \ldots, \bar{\mathbf{v}}_m$ are $(T_1, 1)$-periodic.

Proof:

Let $\bar{w}_j := w_j$ for $j = 1, \ldots, m$ and $\bar{t}_2 := t_2 + \int_0^{t_1} w_0(s) - \bar{w}_0(s) \, \mathrm{d}s$. Using the chain rule of differentiation, we obtain with (35) and $\mu_{li0} = \delta_{li}$

$$\begin{aligned}
& A \left[\frac{\partial \bar{\mathbf{v}}_l}{\partial t_1}(t_1, t_2) + \sum_{i,j=0}^{m} \mu_{lij} \bar{w}_j(t_1) \frac{\partial \bar{\mathbf{v}}_i}{\partial t_2}(t_1, t_2) \right] \\
= \; & A \left[\frac{\partial \hat{\mathbf{v}}_l}{\partial t_1}(t_1, \bar{t}_2) + (w_0(t_1) - \bar{w}_0(t_1)) \frac{\partial \hat{\mathbf{v}}_l}{\partial t_2}(t_1, \bar{t}_2) + \sum_{i,j=0}^{m} \mu_{lij} \bar{w}_j(t_1) \frac{\partial \hat{\mathbf{v}}_i}{\partial t_2}(t_1, \bar{t}_2) \right] \\
= \; & A \left[\frac{\partial \hat{\mathbf{v}}_l}{\partial t_1}(t_1, \bar{t}_2) + \sum_{i,j=0}^{m} \mu_{lij} w_j(t_1) \frac{\partial \hat{\mathbf{v}}_i}{\partial t_2}(t_1, \bar{t}_2) \right] \\
= \; & \mathbf{F}_l(\mathbf{b}(t_1), \hat{\mathbf{v}}(t_1, \bar{t}_2)) \quad = \quad \mathbf{F}_l(\mathbf{b}(t_1), \bar{\mathbf{v}}(t_1, t_2))
\end{aligned}$$

for $l = 0, 1, \ldots, m$. It is straightforward to show that the periodicity of $w_0, \bar{w}_0$ and the condition (36) imply that the MVFs $\bar{\mathbf{v}}_l$ inherit the periodicities of the original MVFs $\hat{\mathbf{v}}_l$. □

Theorem 2 demonstrates that the biperiodic solution of (31) can be transformed to another biperiodic solution involving a different periodic expected value of the local frequency function, where the average coincides. In contrast, the functions $w_1, \ldots, w_m$, which determine the variances of the problem, cannot be modified.

A more precise analysis becomes feasible, if the transformation matrix S in (34) is independent of the slow time scale.

Theorem 3 *If the matrices (33) can be diagonalised via*

$$B(t_1) = S^\top \Lambda(t_1) S \tag{37}$$

with a constant orthogonal matrix $S \in \mathbb{R}^{(m+1)\times(m+1)}$ *and a diagonal matrix* $\Lambda(t_1) = \operatorname{diag}(\lambda_0(t_1), \ldots, \lambda_m(t_1))$*, then the gPC wMPDAE system (32) is equivalent to the system*

$$(I_{m+1} \otimes A)\frac{\partial \tilde{\mathbf{v}}}{\partial t_1} + (\Lambda(t_1) \otimes A)\frac{\partial \tilde{\mathbf{v}}}{\partial t_2} = (S \otimes I_k)\mathbf{F}(\mathbf{b}(t_1), (S^\top \otimes I_k)\tilde{\mathbf{v}}) \tag{38}$$

with $\tilde{\mathbf{v}} := (S \otimes I_k)\hat{\mathbf{v}}$.

Proof:

Multiplying (32) by $S \otimes I_k$ yields

$$(S \otimes I_k)(I_{m+1} \otimes A)\frac{\partial \hat{\mathbf{v}}}{\partial t_1} + (S \otimes I_k)(B(t_1) \otimes A)\frac{\partial \hat{\mathbf{v}}}{\partial t_2} = (S \otimes I_k)\mathbf{F}(\mathbf{b}(t_1), \hat{\mathbf{v}}).$$

Using the rule $(A \otimes B)(C \otimes D) = (AC) \otimes (BD)$ several times, we obtain

$$(I_{m+1} \otimes A)(S \otimes I_k)\frac{\partial \hat{\mathbf{v}}}{\partial t_1} + ((SB(t_1)) \otimes A)\frac{\partial \hat{\mathbf{v}}}{\partial t_2} = (S \otimes I_k)\mathbf{F}(\mathbf{b}(t_1), \hat{\mathbf{v}})$$

and

$$(I_{m+1} \otimes A)(S \otimes I_k)\frac{\partial \hat{\mathbf{v}}}{\partial t_1} + ((SB(t_1)S^\top) \otimes A)(S \otimes I_k)\frac{\partial \hat{\mathbf{v}}}{\partial t_2} = (S \otimes I_k)\mathbf{F}(\mathbf{b}(t_1), \hat{\mathbf{v}})$$

It holds $SB(t_1)S^\top = \Lambda(t_1)$. Finally, the substitution $\tilde{\mathbf{v}} = (S \otimes I_k)\hat{\mathbf{v}}$ or, equivalently, $\hat{\mathbf{v}} = (S^\top \otimes I_k)\tilde{\mathbf{v}}$ yields the formula (38). □

A decoupling has been achieved in the left-hand side of (38). Using the partition $\tilde{\mathbf{v}} = (\tilde{\mathbf{v}}_0^\top, \ldots, \tilde{\mathbf{v}}_m^\top)^\top$, we investigate the structure of the novel system. The set of equations consists of $m+1$ subsystems

$$A\left(\frac{\partial \tilde{\mathbf{v}}_i}{\partial t_1} + \lambda_i(t_1)\frac{\partial \tilde{\mathbf{v}}_i}{\partial t_2}\right) = \mathbf{G}_i(\mathbf{b}(t_1), \tilde{\mathbf{v}}) \qquad \text{for } i = 0, 1, \ldots, m. \tag{39}$$

In the ith subsystem, the left-hand side includes information from the components $\tilde{\mathbf{v}}_i$ only. Moreover, we recognise that the left-hand side agrees with the original wMPDAE formulation (11). Hence $m+1$ families of characteristic curves exist defined by the functions λ_i for $i = 0, 1, \ldots, m$. The characteristic projections of the ith subsystem (39) read, cf. [10],

$$t_2(t_1) = \int_0^{t_1} \lambda_i(s)\, \mathrm{d}s + c \qquad \text{for each } \; c \in \mathbb{R}. \tag{40}$$

For fixed i, the characteristic projections represent a family of parallel curves in the domain of dependence. Accordingly, the system (31) or (32), equivalently, exhibits the structure of a hyperbolic partial differential equation. In case of non-constant transformation matrices S, the type is still hyperbolic, since a decoupling of the left-hand side exists locally due to (34).

An efficient method of characteristics for solving biperiodic problems of the system of wMPDAEs (11) has been constructed in [10]. However, a technique based on the characteristic projections (40) of the system (31) from the gPC is unfavourable in view of the following reasons:

1. Several families of characteristic projections exist in contrast to just one family belonging to the original system (11).

2. The functions $w_0, \ldots, w_m$ are unknowns of the problem (31). On the one hand, eigenvalue problems have to be solved for the determination of the characteristic projections (40). On the other hand, the characteristic projections of the underlying system (11) follow directly from the local frequency function ν.

3. The transformation (34) involves matrices $S(t_1)$ depending on the variable t_1 in general. Thus the system (31) can be decoupled just locally.

4. In case of constant transformation matrices S, the equivalent system (38) is decoupled in the left-hand side only, whereas the right-hand side still includes all components of the solution. The same holds for a locally used transformation (34) in case of non-constant matrices $S(t_1)$.

The above reasons indicate that solving initial value problems of the system (31) by a method of characteristics becomes complicated. Moreover, we consider biperiodic boundary value problems. Hence finite difference methods on axiparallel grids have to be preferred for the numerical solution of a biperiodic problem of a system (31) in time domain. Obviously, a method of characteristics is also unfavourable in case of the more sophisticated system (29) with random matrix A.

5 Illustrative Example

As test example, we apply the electric circuit of a voltage controlled oscillator (VCO) shown in Fig. 2. The circuit consists of a capacitance, an inductance and a nonlinear resistance. The capacitance is controlled by an independent input signal. Mathematical modelling based on a network approach yields the system

$$\begin{aligned} \dot{u} &= \imath_C/(C_0 b(t)) \\ \dot{\imath}_L &= u/L_0 \\ 0 &= \imath_R - g(u) \\ 0 &= \imath_R + \imath_L + \imath_C. \end{aligned} \tag{41}$$

The unknowns are the node voltage and the currents through capacitance, inductance and resistance, respectively. The system (41) represents a semi-explicit system of DAEs with differential index 1. The current-voltage relation of the nonlinear resistance reads

$$g(u) = (G_0 - G_\infty) U_0 \tanh\left(\frac{u}{U_0}\right) + G_\infty u.$$

We set the technical parameters to

$$C_0 = 1 \text{ nF}, \quad L_0 = 1 \ \mu\text{H}, \quad U_0 = 1 \text{ V}, \quad G_0 = -0.1 \text{ A/V}, \quad G_\infty = 0.25 \text{ A/V}.$$

Using a constant input $b \equiv 1$, the VCO (41) exhibits periodic solutions with rate $T_2 \approx 270$ ns. We arrange the slowly varying input signal

$$b(t) = 1 + 0.8 \cos\left(\frac{2\pi}{T_1} t\right) \qquad \text{with } T_1 = 1 \text{ ms}.$$

Now the system (41) exhibits quasiperiodic solutions involving frequency modulation. We apply the corresponding system of wMPDAEs (11) with biperiodic boundary conditions. Numerical simulations of the wMPDAEs (11) using this VCO with a slightly different mathematical modelling are presented in [13].

We assume an uncertainty in the inductance and define the random parameter

$$L(\xi) = L_0(1 + 0.2\xi) \tag{42}$$

with uniformly distributed random variable $\xi \in [-1, 1]$. Thus we employ relatively large perturbations of 20% for demonstration. The according gPC representation (25) of the random field involves the Legendre polynomials as orthonormal basis. We truncate the series at the term $m = 3$, i.e., univariate polynomials up to degree 3 are used. The coupled system (29) of wMPDAEs consists of 16 equations. We use four additional conditions (30) with $\eta_0 = 0$ to determine the unknown coefficient functions of the local frequency function.

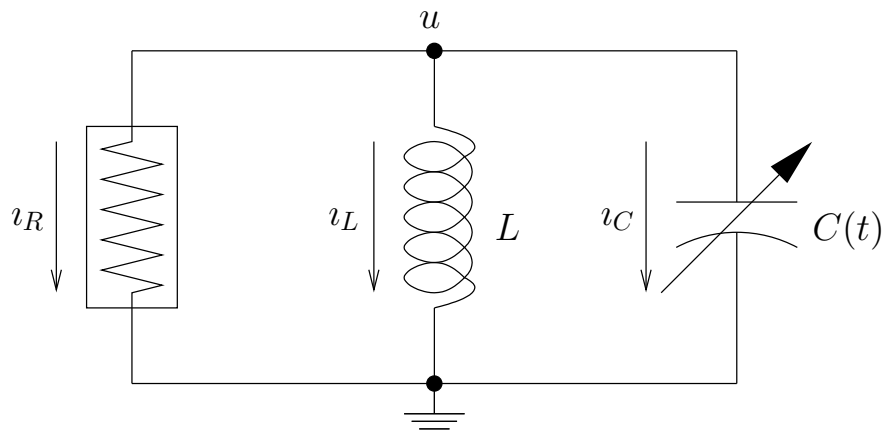

Figure 2: Circuit of voltage controlled oscillator.

A finite difference method yields a numerical solution of the biperiodic boundary value problem for (29) on a uniform grid in the domain $[0, T_1] \times [0, 1]$. Partial derivatives are discretised by asymmetric difference formulas of second order (BDF2). Required evaluations of the right-hand side in (29) are computed by Gauss-Legendre quadrature with $q = 10$ nodes. We apply a grid of 50×50 points, which results in a nonlinear system with 40.000 equations. A Newton iteration converges to the numerical solution, where a deterministic solution of (11) yields the starting values.

We discuss briefly the general computational effort of the finite difference method. Let n_1, n_2 be the number of grid points in each coordinate direction. A nonlinear system $\mathbf{H} = \mathbf{0}$ appears with dimension $n_1 n_2 (m + 1)k$. Assume that expected values (15) are approximated by Gaussian quadrature using q nodes. Each computation of $\mathbf{H}$ and its Jacobian matrix $\mathrm{D}\mathbf{H}$ demands $n_1 n_2 q$ evaluations of $\mathbf{f} \in \mathbb{R}^k$ from (11) and $\mathrm{D}\mathbf{f} \in \mathbb{R}^{k \times k}$, respectively. In the Newton method, the matrices of the linear systems exhibit a band structure except for external blocks due to the periodicity. Assuming $n_1 = n_2 = n$, the computational work of an LU-decomposition is about $\mathcal{O}(n^4 m^3 k^3)$, whereas a dense matrix implies $\mathcal{O}(n^6 m^3 k^3)$. The gPC strategy becomes efficient if a small m is sufficient, say $m \leq 5$. The aim of the MPDAE approach is to achieve good approximations on relatively coarse grids in time domain, say $n \leq 100$. In contrast, the size k of the underlying DAE model (2) depends on the given application.

Fig. 3 illustrates the resulting coefficient functions of the local frequencies according to (28) as well as the corresponding standard deviation calculated analogue to (22). The expected values of the MVFs are shown in Fig. 4. These expected values are similar to the deterministic solution of the underlying wMPDAEs (11). Furthermore, Fig. 5 demonstrates the other coefficient functions of the node volt-

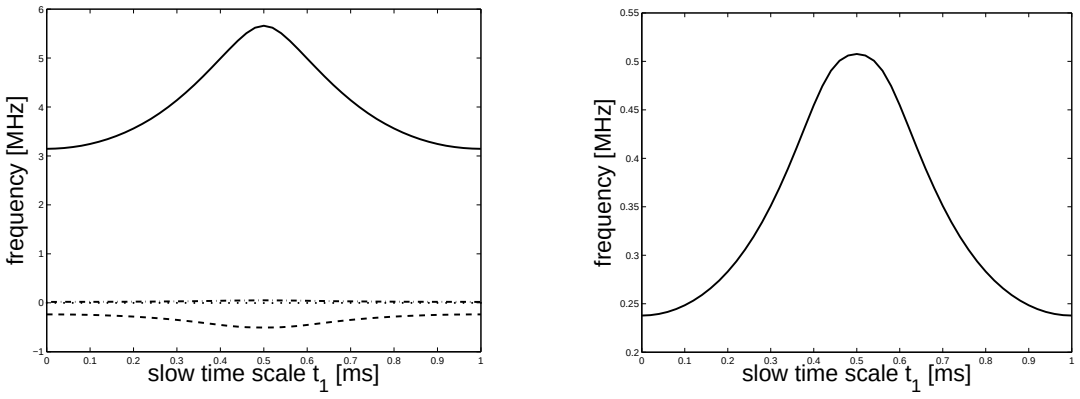

Figure 3: Coefficient functions w_i (left) for $i = 0$ (—), $i = 1$ (- - -), $i = 2$ (- · -), $i = 3$ ($\cdots$) and standard deviation (right) of local frequency function.

Table 1: Maximum values of the coefficient functions from gPC wMPDAE.

	$i = 0$	$i = 1$	$i = 2$	$i = 3$
ν	$5.7 \cdot 10^{6}$	$5.1 \cdot 10^{5}$	$5.0 \cdot 10^{4}$	$4.7 \cdot 10^{3}$
$\hat{u}$	$1.4 \cdot 10^{0}$	$4.7 \cdot 10^{-2}$	$3.4 \cdot 10^{-3}$	$2.7 \cdot 10^{-4}$
$\hat{i}_L$	$7.2 \cdot 10^{-2}$	$2.7 \cdot 10^{-3}$	$2.3 \cdot 10^{-4}$	$2.1 \cdot 10^{-5}$
$\hat{i}_C$	$1.1 \cdot 10^{-1}$	$7.2 \cdot 10^{-3}$	$5.7 \cdot 10^{-4}$	$4.8 \cdot 10^{-5}$
$\hat{i}_R$	$4.1 \cdot 10^{-2}$	$5.4 \cdot 10^{-3}$	$4.5 \cdot 10^{-4}$	$3.9 \cdot 10^{-5}$

age in the expansion (25). Thereby, we recognise the applied additional boundary conditions (30). Finally, approximations of the standard deviations of the MVFs are computed following (22) and displayed in Fig. 6.

Using the computed approximations in the grid points, we show the maximum value of each coefficient function for each component of the solution of (29) in Table 1. The coefficient functions decrease about one order of magnitude for increasing degree, which indicates a relatively fast convergence of the applied gPC expansions. Although the stochastic perturbation (42) of the parameter L_0 is relatively large, the matrices (33) remain positive definite in each grid point, cf. Theorem 1. Nevertheless, indefinite matrices do not cause problems in the used finite difference method.

For comparison, we determine the coefficient functions of the local frequency via stochastic collocation, see [15, 16]. Thereby, we apply Gauss-Legendre quadrature of different orders. For each node, a biperiodic boundary value problem of (11) has to be solved for a specific parameter (42). We use a finite difference method

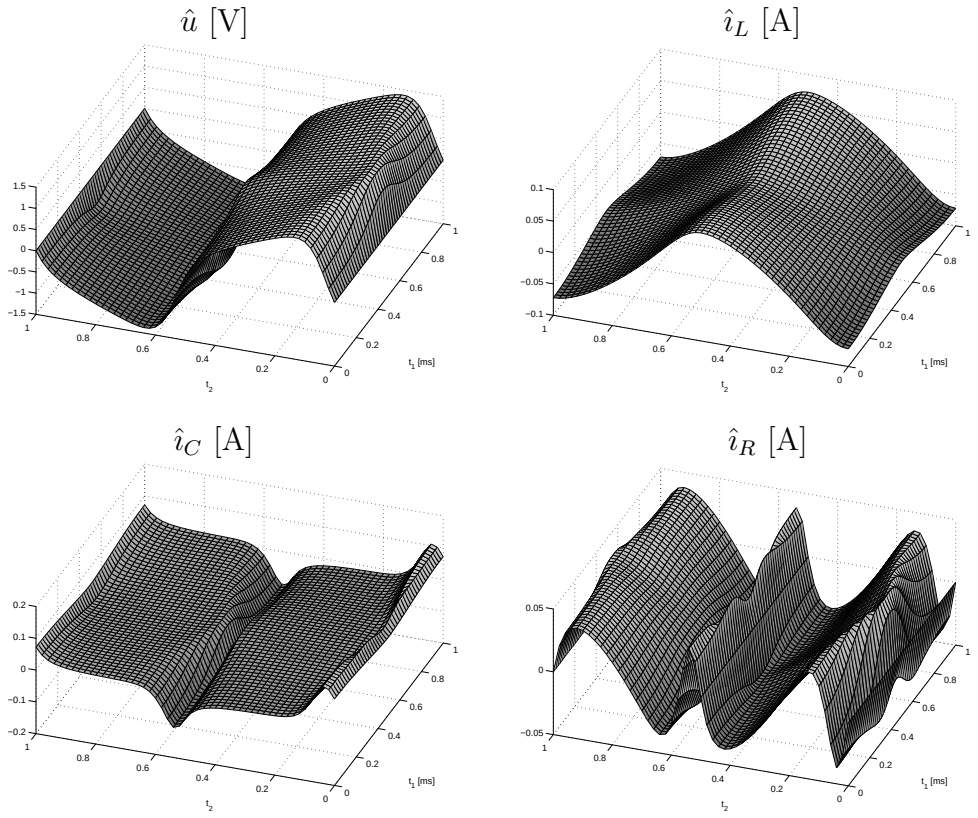

Figure 4: Expected values of the MVFs determined by gPC wMPDAE.

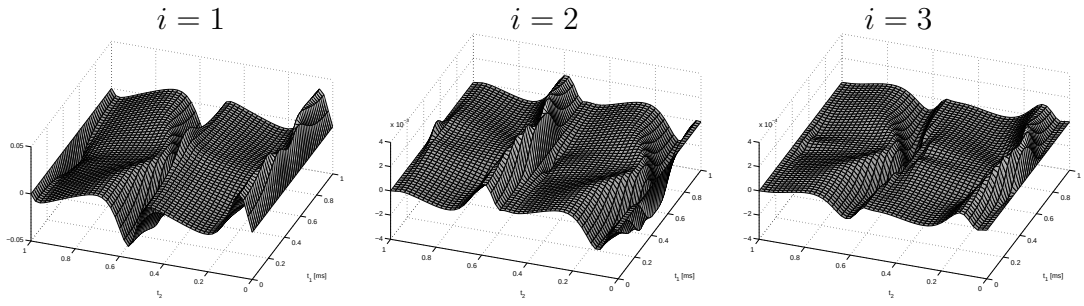

Figure 5: Coefficient functions corresponding to MVF $\hat{u}$ in physical unit [V].

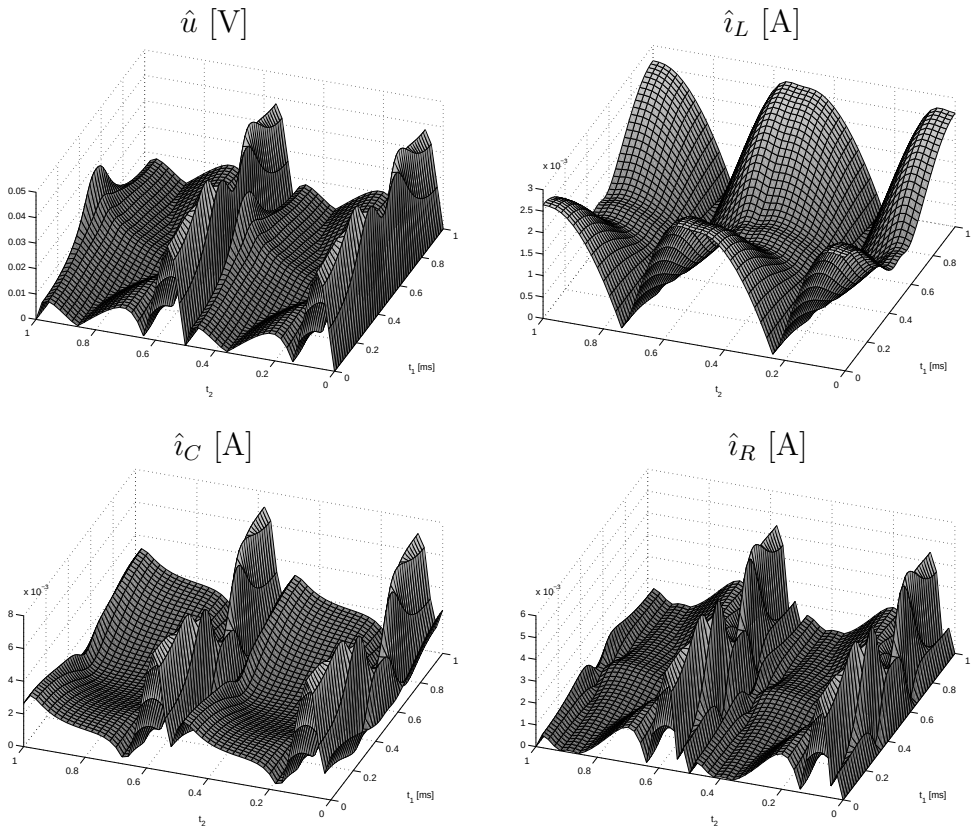

Figure 6: Standard deviations of the MVFs obtained by gPC wMPDAE.

Table 2: Maximum relative differences between numerical solutions of the local frequency obtained by Galerkin gPC system in comparison to stochastic collocation using Gauss-Legendre-quadrature with q nodes.

	w_0	w_1	w_2	w_3
$q = 2$	$8 \cdot 10^{-5}$	$9 \cdot 10^{-3}$	$1 \cdot 10^{0}$	$1 \cdot 10^{2}$
$q = 4$	$2 \cdot 10^{-8}$	$9 \cdot 10^{-7}$	$9 \cdot 10^{-5}$	$1 \cdot 10^{-2}$
$q = 10$	$2 \cdot 10^{-8}$	$1 \cdot 10^{-7}$	$2 \cdot 10^{-5}$	$2 \cdot 10^{-3}$

on a 50×50 grid again, where nonlinear systems including 10.000 equations result. Table 2 illustrates the differences of the resulting coefficient functions in comparison to the previously computed solution of (29). The values represent relative differences, where the maximum difference is divided by the maximum value of each component. The relative differences decrease for higher orders of the used quadrature. The coefficient functions of the MVFs exhibit the same behaviour. The decreasing differences indicate that we have computed a correct solution of the wMPDAEs (29) from the gPC approach.

For an additional verification, we arrange a classical Monte-Carlo simulation of the stochastic model. We determine s samples of the random variable (42) using pseudo random numbers for $\xi \in [-1, 1]$. The biperiodic boundary value problem of the wMPDAEs (11) is solved by the finite difference method on a 50×50 grid again. Thus s independent nonlinear systems appear in this Monte-Carlo simulation. We calculate the mean values and the sample variances to achieve approximations of the expected values and the standard deviations in case of $s = 100$ as well as $s = 1000$. The previously computed solution of the gPC wMPDAEs (29), which results from the Galerkin approach, yields alternative approximations via (22). We determine the maximum absolute differences on the grid for each component separately, see Table 3. We recognise that the differences decrease for larger numbers of samples. Since the discrepancies become also small in a relative sense, the correctness of the solution from the gPC approach is confirmed.

For the sake of shortness, we omit the reconstruction of data corresponding to solutions of the DAEs (2) via the computed solution of the gPC wMPDAEs (29).

Table 3: Maximum absolute differences in expected values and standard deviations between the solution from gPC and solutions from a Monte-Carlo simulation using s samples. Results are given for each component separately.

	expected values		standard deviations	
	$s = 100$	$s = 1000$	$s = 100$	$s = 1000$
ν	$4.7 \cdot 10^{4}$	$2.1 \cdot 10^{3}$	$3.1 \cdot 10^{4}$	$2.0 \cdot 10^{3}$
$\hat{u}$	$4.1 \cdot 10^{-3}$	$1.7 \cdot 10^{-4}$	$2.3 \cdot 10^{-3}$	$1.7 \cdot 10^{-4}$
$\hat{i}_L$	$2.5 \cdot 10^{-4}$	$1.1 \cdot 10^{-5}$	$1.5 \cdot 10^{-4}$	$1.0 \cdot 10^{-5}$
$\hat{i}_C$	$6.3 \cdot 10^{-4}$	$2.7 \cdot 10^{-5}$	$3.6 \cdot 10^{-4}$	$2.6 \cdot 10^{-5}$
$\hat{i}_R$	$4.7 \cdot 10^{-4}$	$2.0 \cdot 10^{-5}$	$2.7 \cdot 10^{-4}$	$2.0 \cdot 10^{-5}$

6 Conclusions

The concept of MPDAEs provides an alternative simulation of DAEs including quasiperiodic solutions. Assuming random parameters, we applied the strategy of the generalised polynomial chaos to the systems of MPDAEs. Thereby, a Galerkin approach yields larger coupled systems of MPDAEs, which inherit a hyperbolic structure. Coupled systems of MPDAEs reproducing amplitude modulated signals exhibit the form of the underlying multirate system. Hence a method of characteristics can be used efficiently. In contrast, coupled systems resulting from warped MPDAEs, which describe the case of frequency modulated signals, become more involved. We analysed the structure of characteristic curves of these coupled systems. It follows that a method of characteristics is unfavourable due to several reasons, although a corresponding algorithm may be feasible. Nevertheless, finite difference methods solve the coupled systems of MPDAEs appropriately on uniform grids in time domain.

Acknowledgements
The author has been supported within the PostDoc programme of 'Fachgruppe Mathematik und Informatik' from Bergische Universität Wuppertal (Germany).

References

[1] F. Augustin, A. Gilg, M. Paffrath, P. Rentrop and U. Wever, Polynomial chaos for the approximation of uncertainties: chances and limits, Euro. Jnl. of Applied Mathematics 19 (2008) 149-190.

[2] H.G. Brachtendorf, G. Welsch, R. Laur and A. Bunse-Gerstner, Numerical steady state analysis of electronic circuits driven by multi-tone signals, Electrical Engineering 79 (1996) 103-112.

[3] Y. Cao, Z. Chen and M. Gunzburger, ANOVA expansions and efficient sampling methods for parameter dependent nonlinear PDEs. Int. J. Numer. Anal. Mod. 6 (2009) 256-273.

[4] R.G. Ghanem and P.D. Spanos: Stochastic Finite Elements, Dover Publications Inc., Mineola, New York, 2003.

[5] M. Günther and U. Feldmann, CAD based electric circuit modeling in industry I: mathematical structure and index of network equations, Surv. Math. Ind. 8 (1999) 97-129.

[6] W. Kampowsky, P. Rentrop and W. Schmitt, Classification and numerical simulation of electric circuits, Surv. Math. Ind. 2 (1992) 23-65.

[7] G.E. Karniadakis, C.H. Su, D. Xiu, D. Lucor, C. Schwab and R.A. Todor, Generalized polynomial chaos solution for differential equations with random inputs, Research Report No. 2005-01, ETH Zürich, 2005.

[8] O. Narayan and J. Roychowdhury, Analyzing oscillators using multitime PDEs, IEEE Trans. CAS I 50 (2003) 894-903.

[9] R. Pulch and M. Günther, A method of characteristics for solving multirate partial differential equations in radio frequency applications, Appl. Numer. Math. 42 (2002) 397-409.

[10] R. Pulch, Multi time scale differential equations for simulating frequency modulated signals, Appl. Numer. Math. 53 (2005) 421-436.

[11] R. Pulch, Warped MPDAE models with continuous phase conditions, in: A. Di Bucchianico, R.M.M. Mattheij and M.A. Peletier, (Eds.), Progress in Industrial Mathematics at ECMI 2004, Mathematics in Industry, Vol. 8, Springer, Berlin, 2006, pp. 179-183.

[12] R. Pulch, M. Günther and S. Knorr, Multirate partial differential algebraic equations for simulating radio frequency signals, Euro. Jnl. of Applied Mathematics 18 (2007) 709-743.

[13] R. Pulch, Transformation qualities of warped multirate partial differential algebraic equations, in: M. Breitner, G. Denk and P. Rentrop, (Eds.), From Nano to Space - Applied Mathematics Inspired by Roland Bulirsch, Springer, Berlin, 2008, pp. 27-42.

[14] J. Roychowdhury, Analysing circuits with widely-separated time scales using numerical PDE methods, IEEE Trans. CAS I 48 (2001) 578-594.

[15] D. Xiu and J.S. Hesthaven, High order collocation methods for differential equations with random inputs, SIAM J. Sci. Comput. 27 (2005) 1118-1139.

[16] D. Xiu, Efficient collocation approach for parametric uncertainty analysis, Comm. Comput. Phys. 2 (2007) 293-309.